Box Girder Bridge Design—State of the Art

C. P. HEINS

The information that will be presented herein will pertain to straight and curved steel composite box girder bridges of moderate span length (50–250 ft) that are utilized for highway interchanges. Although the general theories are applicable to larger structures, the design formulas that have been developed and will be given herein are only suitable for the conventional highway bridge.

BRIDGE TYPE

Details—During the past two years, the ASCE Task Committee on Horizontally Curved Steel Box Girder Bridges has conducted a comprehensive survey[1] on the details of box girder bridges (straight and curved). This survey has shown that the number of box girder bridges being built has increased dramatically since 1961, as shown in Fig. 1.

The collected details (geometry) of the 82 reported bridges has been reduced to those shown in Tables 1–3, with the ratios of these dimensions given in Tables 4–6. The various parameters listed in these tables are shown in Fig. 2. These bridges represent typical steel-composite structures, and the data given therein can be used for preliminary design. The bridges generally have internal cross-bracing and top lateral bracing with external diaphragms placed only at the support piers.

Section Geometry—In the design of any complex structure in which the section changes and the forces are not readily computed, it is useful to have data or empirical relationships to select plate and girder sizes. Examination of the data presented in Tables 1–3 has resulted in the following general equations:

Single Span:

$$A_T = 10d\left(1 - \frac{84}{L}\right) \tag{1}$$

$$A_B = 12.9d\left(1 - \frac{92}{L}\right) \tag{2}$$

where

A_T, A_B = total area of the top and bottom flange, respectively, in.^{2}
L = span length, ft ($90 \leq L \leq 200$)
d = girder depth, in.

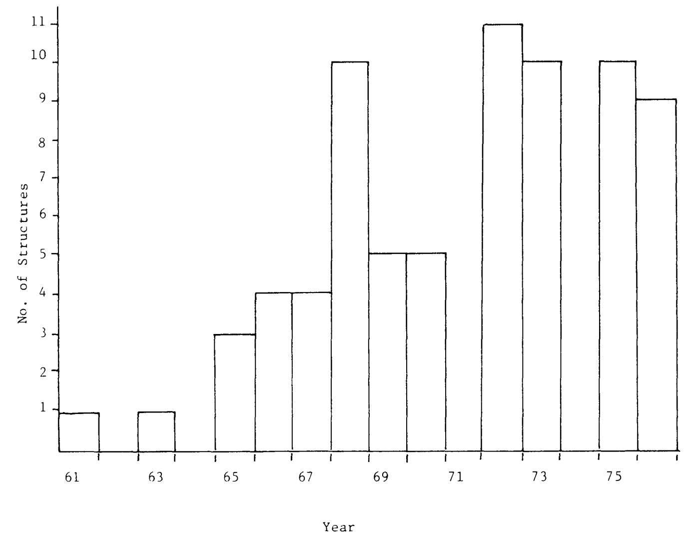

Fig. 1. Frequency of box girder bridge built vs. year built

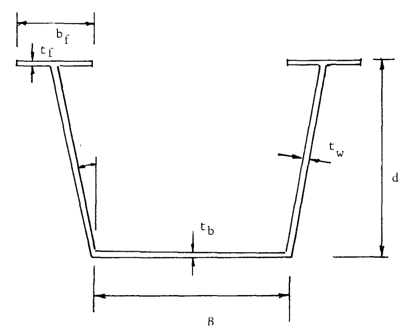

Fig. 2. Box girder dimensions

C. P. Heins is Professor of Civil Engineering, University of Maryland, College park, Md.

Ed. Note: This paper was originally presented at the AISC National Engineering Conference, Los Angeles, Calif., in May 1978.

Table 1. Single-Span Box Bridge Dimensions

L (ft)	N_B	W_R (ft)	R (ft)	d (in.)	B (in.)	t_b (in.)	t_w (in.)	b_f (in.)	t_f (in.)	θ (deg)	Brace Spac'g (ft)
90	1	6.6	300	36.6	50	$\frac{1}{2}$	$\frac{1}{2}$	12	$\frac{7}{8}$	0	a
109.6	2	12–16	760	52	72	$1\frac{3}{8}$	$\frac{5}{8}$	18	1	0	11
118.5	4	43–48	1773.8 560.5	48	60	$\frac{1}{2}$	$\frac{1}{2}$	18	1	0	a
140	4	55.6	600	120	56	2	$\frac{3}{4}$	24	$1–2\frac{1}{4}$	13.6	25
177	4	55.6	2000	120	56	$2\frac{5}{8}$	$\frac{3}{4}$	24	$2–2\frac{5}{8}$	13.6	25
208	5	78.8	0	77	61	2	$\frac{1}{2}$	24	2	13.2	23–26

[a]Not known.

In addition to developing Eqs. (1) and (2), the following general trends were noted:

1. Web thickness varied from $\frac{1}{2}$-in. to $\frac{3}{4}$-in.
2. The ratio of roadway width in feet, W_R, to number of boxes, N_B, varied as $6.5 \leq W_R/N_B \leq 16.0$, with an average of 12.0.
3. Width of box varied between 50 in. and 72 in.
4. Maximum thickness of bottom flange was 2 in.
5. Width of top flange varied as $W_F = 0.12(L - 100) + 12$ with a minimum of 12 in.
6. Maximum thickness of top flange was $2\frac{5}{8}$ in.
7. Minimum ratio d/L was 1/30, with an average of 1/23.

Table 2. Two-Span Continuous Box Bridge Dimensions

L (ft)	N_B	W_R (ft)	R (ft)	d (in.)	B (in.)	t_b (in.)	t_w (in.)	b_f (in.)	t_f (in.)	θ (deg)	Brace Spac'g (ft)	F_y (ksi)
100 100	3	44	∞	48	72	$+1\frac{1}{2}$ $-\frac{3}{4}$	$\frac{3}{8}$	+12 −17	$+\frac{1}{2}$ $-1\frac{1}{2}$	a	a	36
108 108	2	30	162.5	48	57	$+\frac{5}{16}$ $-\frac{1}{2}$	$\frac{3}{8}$	14	$\frac{5}{8}$	26	15	50
111 111	2	42	2885	42	114	$+\frac{1}{2}$ $-\frac{7}{8}$	$\frac{3}{8}$	+12 −18	$+1\frac{1}{2}$ $-2\frac{1}{4}$	8	15	50
120 120	3	44	∞	58	68	$+\frac{5}{8}$ $-\frac{7}{8}$	$\frac{3}{8}$	+14 −19	$+\frac{3}{8}$ $-1\frac{1}{2}$	a	a	36
120 120	2	42	1637	56	108	$+\frac{7}{16}$ $-\frac{5}{8}$	$+\frac{7}{16}$ $-\frac{5}{8}$	+21 −24	+1 $-1\frac{1}{4}$	9	16–8	50
145 145	3	43	∞	60	56	$+\frac{11}{16}$ $-\frac{3}{4}$	$\frac{7}{16}$	14	$+\frac{15}{16}$ $-1\frac{1}{2}$	0	a	50
145 145	3	43	∞	60	56	$+\frac{5}{8}$ $-\frac{11}{16}$	$\frac{3}{8}$	14	$+\frac{5}{8}$ $-\frac{13}{16}$	0	a	50
174 174	2	38	2272	71	101	$+\frac{1}{2}$ $-\frac{3}{4}$	$\frac{3}{8}$	18 18	$+1\frac{1}{4}$ $-2\frac{1}{2}$	9	24	50
185 185	2	55.6	∞	120	56	$+1\frac{1}{2}$ $-2\frac{1}{2}$	$+\frac{3}{4}$ −1	+24 −66	+1 $-1\frac{1}{8}$	0	a	36
194 214	3	42	2884	63	86	$+1\frac{1}{2}$ $-2\frac{1}{4}$	$\frac{3}{8}$	24	$2\frac{1}{4}$	0	12	36
217 217	2	55.6	2000	120	56	$+2\frac{1}{2}$ $-2\frac{7}{8}$	$+\frac{3}{4}$ −2	+24 −66	$+1\frac{3}{4}$ $-1\frac{5}{8}$	0	a	36
220 220	2	55.6	2000	120	56	$+2\frac{5}{8}$ $-3\frac{1}{8}$	$+\frac{3}{4}$ −2	+24 −66	$+1\frac{15}{16}$ $-1\frac{7}{8}$	13.6	a	36

Note: + indicates positive moment region. − indicates negative moment region.
[a]Not known.

Two Span:

The total plate areas of a two span bridge, shown in Fig. 3, are computed as:

$$A_B{}^+ = \frac{1}{K}(0.00153L^2 - 0.223L + 13) \tag{3}$$

$$A_B{}^- = 1.17\, A_B{}^+ \frac{F_y{}^-}{F_y{}^+} \tag{4}$$

$$A_T{}^+ = 0.64\, A_B{}^+ \tag{5}$$

$$A_T{}^- = 1.6\, A_B{}^+ \frac{F_y{}^-}{F_y{}^+} \tag{6}$$

where

$A_B{}^+, A_B{}^-$, $A_T{}^+, A_T{}^-$ = total bottom and top flange areas (in.^{2}) in the positive (+) and negative (−) moment regions, as shown in Fig. 3

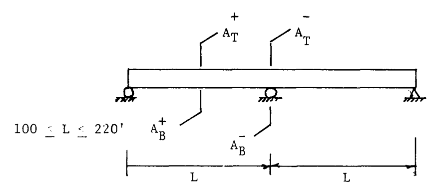

Fig. 3. Two-span box girder bridge—flange area locations

F_y = yield point of material, ksi, at section being examined
L = span length, ft ($100 \le L \le 220$)
K = $N_B F_y d/(W_R \times 600)$, where F_y is at $A_B{}^+$
W_R = roadway width, ft
N_B = number of boxes

Table 3. Three-Span Continuous Box Bridge Dimensions

L (ft)	N_B	W_R (ft)	R (ft)	d (in.)	B (in.)	t_b (in.)	t_w (in.)	b_f (in.)	t_f (in.)	θ (deg)	Brace Spac'g (ft)	n	F_y (ksi)
90 120 90	2	44	716	41	94	7/8	3/8	+14 −22	+ 3/4 −1	0	18[b] 24	1.33	+36 −50
93 124 93	2	38	2845	42	114	+ 1/2 − 7/8	3/8	+12 −16	+ 7/8 −1	9.5	15	1.33	50
102 102 102	2	25	650	51	55 1/2	+ 7/8 − 7/8 + 1/2	− 3/8	*a*	*a*	14	10.3	1.0	36
104 160 104	2	38	5730	61	108	+ 3/4 −1	7/16	+16 −16	+1 −2	9.5	15	1.54	50
100 132 122	2	43	1310	54	106 1/2	+ 3/4 −1	+ 3/8 − 1/2	+24 −30	+1 1/4 −1 3/4	14	*a*	1.08	36
116 131 116	2	33	∞	63	81 3/4	+ 3/8 − 3/4	3/8	14	+ 3/4 −1 1/2	*a*	*a*	1.13	*a*
166 206 166	4	68.5	1000	55	78	+1 1/4 −2 1/4 +1	5/8	+20 −30 +20	+1 5/8 −3 +1 5/8	8	20.6	1.24	50
173 196 172	3	40.5	760	60	92	+1 1/4 −1 1/4 +1	+ 7/8 − 1/2	+20 −24 +20	+1 3/4 −2 1/4 +1	0	*a*	1.14	+36 −50
174 282 125	2	55.6	2000	120	56	+1 −3 1/8 +3 1/8	+ 3/4 −2	+24 −69	+1 −1 7/8	13.6	*a*	1.62	36
100 100 100	2	Var.	874	120	48	+ 5/8 − 9/16	+ 3/8 − 9/16	16	+1 −2	0	10	1.0	+36 −44

Note: + indicates positive moment region. − indicates negative moment region.

[a]Not known.

[b]At end.

The general data indicates that:

1. Web thickness, t_w, varied from $3/8$-in. to $3/4$-in.
2. W_R/N_B varied as $14 \leq W_R/N_B \leq 28$, with an average of 20.
3. Width of box B, in inches, varied approximately as $B = 2.5[(W_R/N_B) - 11]$, with W_R in inches, and $B \geq 55$ in.
4. Width of top flange, b_f, varied from 12 in. to 24 in., in accordance with $b_f^+ = 0.12(L - 100) + 12$.
5. Top flange thickness t_f was less than $2\frac{1}{2}$ in. in all cases.
6. $(d/L)_{min} = 1/30$, with $(d/L)_{avg} = 1/25$.

Table 4. Single-Span Box Bridge Geometric Ratios

L (ft)	d/L	L/R	L/t_b	d/B	B/t_b	b_f/t_f
90	0.0339	0.300	2160	0.732	100	13.7
109.6	0.0395	0.144	956.4	0.722	52.4	12.0
118.5	0.0338	0.211	2844	0.800	120	18.0
140	0.0714	0.233	840	2.14	28	10.7
177	0.0565	0.0885	679.2	2.14	17.9	9.14
208	0.0308	0	1248	1.26	30.5	12.0

Table 5. Two-Span Continuous Box Bridge Geometric Ratios

L (ft)	d/L	L/R	L/t_b	d/B	B/t_b	b_f/t_f
100	0.040	0	2400	0.667	+144	+24
100					−96	−11.3
108	0.0370	0.665	4152	0.842	+182	+22.4
108					−114	−22.4
111	0.0315	0.0385	2664	0.368	+228	+8.0
111					−130	−8.0
120	0.0403	0	2304	0.853	+109	+22.4
120					−77.7	−12.7
120	0.0389	0.0733	3288	0.519	+247	+21.0
120					−173	−19.2
145	0.0345	0	2532	1.07	+81.5	+14.9
145					−74.7	−9.3
145	0.0345	0	2784	1.07	+89.6	+22.4
145					−81.5	−17.2
174	0.0340	0.0766	4176	0.703	+202	+14.4
174					−135	−7.2
185	0.0573	0	1476	2.14	+37.3	+24.0
185					−24.9	−Closed
194	0.0263	0.0707	1596	0.733	+57.3	+10.7
214					−38.2	−10.7
217	0.0461	0.109	1157	2.14	+24.9	+13.7
217					−19.5	−Closed
220	0.0454	0.110	1006	2.14	+21.3	+12.4
220					−17.9	−Closed

Three Span:

The total plate areas of a three span bridge shown in Fig. 4 are computed as:

$$A_T^+ = \frac{n}{6.4K}(L_1 - 73) \tag{7}$$

$$A_B^+ = \frac{n}{5K}(L_1 - 52) \tag{8}$$

$$A_T^- = \frac{n}{2.6K}(L_1 - 100) \tag{9}$$

$$A_B^- = \frac{1}{Kn}(0.964L_2 - 1.65(10^{-3}/L_2^2) - 70) \tag{10}$$

$$A_T^+ = 0.95\,A_T^- - 0.011(A_T^-)^2 - 5.4/K \tag{11}$$

$$A_B^+ = \frac{n}{10K}(L_2 - 48) \tag{12}$$

Table 6. Three-Span Continuous Box Bridge Geometric Ratios

L	d/L	L/R	L/t_b	d/B	B/t_b	b_f/t_f
90	0.0285	0.168	1644	0.436	107.4	+18.7
120						−14.7
90						
93	0.0283	0.0436	2976	0.368	+228	+13.7
124						−9.85
93						
102	0.0417	0.157	2448	0.919	+63.4	a
102					−63.4	
102					+111	
104	0.0318	0.0279	2556	0.565	+144	+16.0
160					−108	−8.0
104						
100	0.0341	0.101	2114	0.507	+142	+19.2
132					−107	−17.1
122						
116	0.0401	0	4188	0.771	+218	+18.7
131					−109	−9.33
116						
166	0.0223	0.206	2472	0.705	+62.4	+12.3
206					−34.7	−10.0
166					+78.0	+12.3
173	0.0253	0.261	2376	0.652	+73.6	+11.4
198					−73.6	−10.7
172					+92.0	+20.0
174	0.0355	0.141	1082	2.14	+56.0	+24.0
282					−17.9	−36.8
125					+17.9	
100	0.100	0.114	2136	2.5	+76.8	+16.0
100					−85.3	−8.0
100						

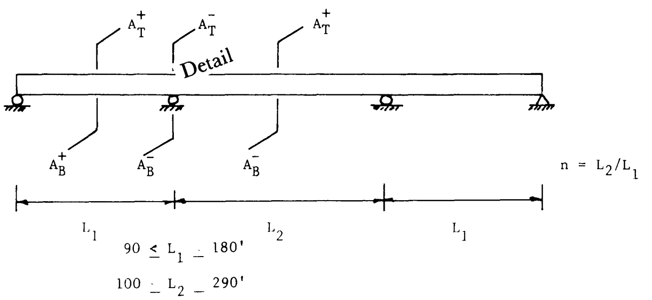

Fig. 4. Three-span box girder bridge—flange area locations

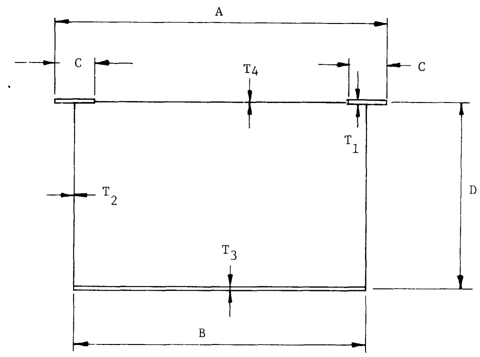

Fig. 5. Actual braced section

where

$90 \leq L_1 \leq 180$ (ft)
$100 \leq L_2 \leq 290$ (ft)
$n = L_2/L_1$
$K = \dfrac{N_B(F_y)d}{(W_R \times 600)}$
F_y = specified yield point of material at section being examined

A study of the data indicates that:

1. Web thickness, t_w, varies from 3/8-in. to 7/8-in.
2. W_R/N_B varies as $12.5 \leq W_R/N_B \leq 22$, with an average of 18.0.
3. The width of the box varies as $B = 7.43[(W_R/N_B) - 5.0]$, with $B_{min} = 55$ in. and $B_{max} = 114$ in.
4. The top flanges had geometry of $3/4 \leq t_f \leq 3$ and $12 \leq b_f \leq 30$.
5. $(d/L_2)_{min} = 1/40$ with $(d/L_2)_{avg} = 1/30.5$.

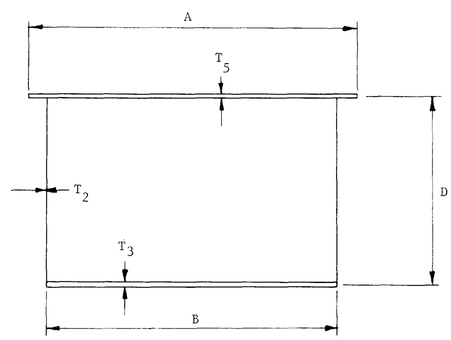

Fig. 6. Modeled braced section

LOAD DISTRIBUTION

Straight Bridges—the AASHTO specification[2] provides design criteria for evaluation of the induced bending moment in straight composite multi-box girder bridges of moderate length. This provision, based on research work by Mattock[3] and the box girder geometry listed in Tables 7 and 8 and Figs. 5–8, is Sect. 1.7.103:

"The live load bending moment for each box girder shall be determined by applying to the girder the fraction W_L of a wheel load (front and rear) according to the following:"

$$W_L = 0.1 + 1.7R + \frac{0.85}{N_w} \tag{13}$$

where

$$R = \frac{N_w}{\text{number of box girders}}, \quad 1.5 \geq R \geq 0.5$$

$N_w = W_c/12$, reduced to nearest whole number
W_c = roadway width between curbs, ft

Curved Bridges—If the bridge system is composed of curved box girders, then resistance of these elements to the applied live load is accomplished by interaction of torsion and bending. This interaction creates a highly indeterminate situation and, in general, requires utilization of a computer program.[4] In order to minimize the need for a computer solution, the response of the typical composite sections, shown in Figs. 7 and 8 and Tables 9 and 10, have been studied when subjected to live loading with the radius $200 \leq R \leq 10{,}000$ ft. The resulting maximum moments were then related to those in the straight system as a function of W_L, as given by Eq. (13). The resulting equation is:

$$W_{L_c} = (1440X^2 + 4.8X + 1)W_L \tag{14}$$

where

W_{L_c} = curved girder load distribution for moment
W_L = straight girder load distribution
$X = 1/R$
R = center line radius of bridge system, ft

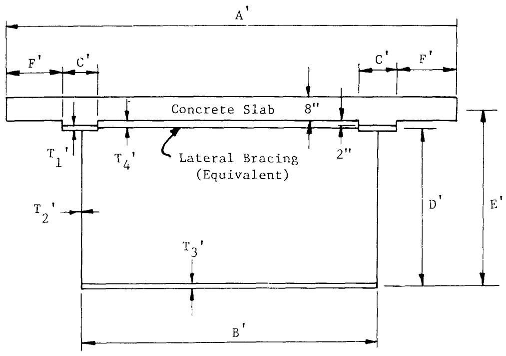

Fig. 7. Actual composite section

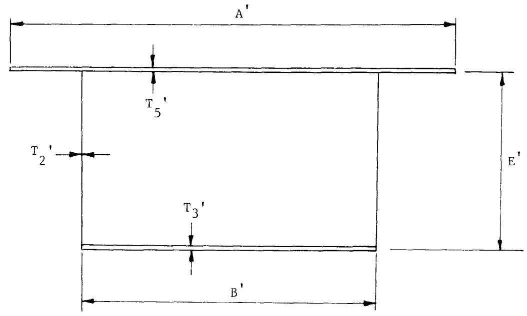

Fig. 8. Modeled composite section

ESTIMATED CURVED GIRDER FORCES

The effect that curvature has on the internal bending moment of a box section, when subjected to truck live load, can be determined readily by using Eqs. (13) and (14). The determination of dead load moment for a curved simple span box can also be readily determined by applying the following.

Dead Load

Bending—The dead load bending moment[5,6] is evaluated from:

$$M_c = (KD)(wL^2/8) \tag{15}$$

where

$$KD = 1 + \frac{1}{10(R/L)^2}$$

Table 7. Dimensions of Braced Sections

Bridge Type	Span (ft)	Dimensions (in.)								
		A	*B*	*C*	*D*	*T1*	*T2*	*T3*	*T4*	*T5*
2L 2G		108	96	12	19.44	0.625	0.375	0.5	0.0878	0.217
3L 3G	50	98	86	12	19.47	0.5625	0.375	0.5	0.0980	0.224
4L 4G		92	80	12	19.50	0.5	0.375	0.5	0.105	0.222
2L 2G		110	96	14	48.125	1.0	0.5	0.75	0.0878	0.331
3L 3G	100	99	86	13	48.125	1.0	0.4375	0.75	0.0980	0.348
4L 4G		92	80	12	48.125	1.0	0.4375	0.75	0.105	0.352
2L 2G		110	96	14	74.75	1.5	0.625	1.0	0.0878	0.458
3L 3G	150	99	86	13	74.75	1.5	0.5625	1.0	0.0980	0.479
4L 4G		92	80	12	74.75	1.5	0.5625	1.0	0.105	0.483

Table 8. Dimensions of Composite Sections

Bridge Type	Span (ft)	Dimensions (in.)										
		A'	*B'*	*C'*	*D'*	*E'*	*F'*	*T1'*	*T2'*	*T3'*	*T4'*	*T5'*
2L 2G		192	96	12	19.44	25.75	42.0	0.625	0.375	0.5	0.0878	0.947
3L 3G	50	172	86	12	19.47	25.75	37.0	0.5625	0.375	0.5	0.0980	0.955
4L 4G		160	80	12	19.50	25.75	34.0	0.5	0.375	0.5	0.105	0.958
2L 2G		192	96	14	48.125	54.625	41.0	1.0	0.5	0.75	0.0878	1.019
3L 3G	100	172	86	13	48.125	54.625	36.5	1.0	0.4375	0.75	0.0980	1.030
4L 4G		160	80	12	48.125	54.625	34.0	1.0	0.4375	0.75	0.105	1.033
2L 2G		192	96	14	74.75	81.5	41.0	1.5	0.625	1.0	0.0878	1.092
3L 3G	150	172	86	13	74.75	81.5	36.5	1.5	0.5625	1.0	0.0980	1.106
4L 4G		160	80	12	74.75	81.5	34.0	1.5	0.5625	1.0	0.105	1.108

L = span length, ft
R = radius to center line of box, ft
w = dead load per unit of length

Torsion—The induced torsional dead load force can similarly be determined by:

$$T_c = (0.75e)(wL) \tag{16}$$

where e = center line offset of the curved box.

Live Load

Torsion—The live load bending effect is found by Eqs. (13) and (14). The torsional force is estimated as follows:

$$T_c = 72N_T(0.95e + \overline{X}) \tag{17}$$

where 72 represents the gross weight of AASHTO truck, and

N_T = number of trucks on box
$\overline{X}$ = eccentricity from center line of box to resultant of laterally positioned trucks
e = center line offset of curved box

Table 9. Section Properties of Modeled Braced Sections

Bridge Type	Span (ft)	Y (in.)	I_x (in.^{4})	K_T (in.^{4})	I_w (in.^{6})	D_w (in.^{6})
2L 2G		6.94	6,550	18,900	3,220,000	1,620,000
3L 3G	50	7.16	6,090	17,000	2,200,000	1,230,000
4L 4G		7.21	5,720	15,600	1,710,000	1,020,000
2L 2G		18.6	67,400	140,000	9,450,000	18,400,000
3L 3G	100	18.9	61,700	118,000	2,940,000	13,500,000
4L 4G		19.1	58,300	107,000	1,720,000	11,100,000
2L 2G		30.3	236,000	378,000	3,710,000	68,000,000
3L 3G	150	30.7	216,000	311,000	216,000	49,500,000
4L 4G		31.0	205,000	280,000	528,000	41,300,000

Table 10. Section Properties of Modeled Composite Sections

Bridge Type	Span (ft)	Y (in.)	I_x (in.^{4})	K_T (in.^{4})	I_w (in.^{6})	D_w (in.^{6})
2L 2G		19.8	27,200	56,800	3,640,000	8,280,000
3L 3G	50	19.8	24,700	49,100	2,170,000	6,140,000
4L 4G		19.7	23,100	44,600	1,540,000	5,050,000
2L 2G		37.8	178,000	250,000	15,800,000	67,800,000
3L 3G	100	37.9	159,000	197,000	16,400,000	48,400,000
4L 4G		37.8	150,000	176,000	15,400,000	40,100,000
2L 2G		52.1	511,000	551,000	98,700,000	228,000,000
3L 3G	150	52.3	460,000	433,000	101,000,000	164,000,000
4L 4G		52.1	433,000	385,000	92,400,000	137,000,000

I_x = bending stiffness
K_T = pure torsional constant
I_w = warping constant
D_w = distortional constant

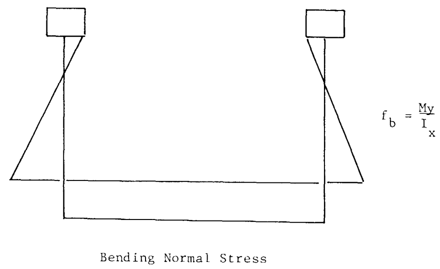

Fig. 9. Bending normal stress

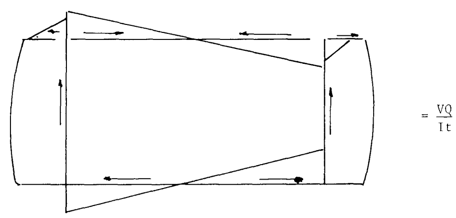

Fig. 10. Bending shearing stress

BENDING AND TORSIONAL STRESSES

Straight Bridges—A straight box girder, when subjected to live loads, will develop bending stresses. The inducement of torsional stresses may occur when the loading is eccentric to the shear center. However, in general, such effects are neglected. Thus the stresses that are considered are:

$$f_b = M/S \tag{18}$$

and

$$\tau = VQ/It \tag{19}$$

where

M = induced bending moment in the box
S = section modulus
V = induced bending shears in the box
Q = statical moment
I = moment of inertia
t = plate thickness

These typical stresses are shown in Figs. 9 and 10.

Curved Bridges—As in the case of straight bridges, curved bridges will develop bending stresses. However, due to the curvature of the bridge, torsional forces will also develop; the magnitude of these will depend on the cross-sectional geometry, span length, and radius.

Pure Torsion—Any section, open or closed, when subjected to a torsional loading, will resist (in part) the applied torque by pure torsion given by:

$$T_{PT} = GK_T\phi' \tag{20}$$

where

K_T = torsion constant
G = shear modulus
ϕ' = rate of change of rotation per unit length

Equation (19) is probably more familiar in the following form:

$$T = GK_T \frac{\phi}{L} \text{ or } \phi = TL/GK_T$$

as given in texts on strength of materials.

The evaluation of the torsion constant K_T is dependent on whether the box section is open or completely closed, where "closed" would represent a composite or braced section. The determination of K_T is given[7] by the following:

Open box:

$$K_T = \frac{1}{3} \sum bt^3 \tag{21}$$

where

b = larger plate dimension
t = smaller plate dimension for same element

Closed box:

$$K_T = 4A_0^2/\oint \frac{ds}{t} \tag{22}$$

where

A_0 = enclosed area of box section, wR to center line of elements
ds = length of a given element
t = corresponding thickness of that element

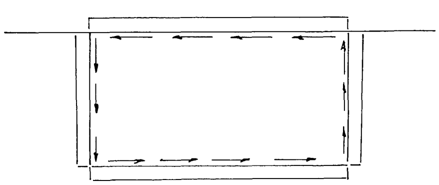

Fig. 11. Pure shearing stress, τ_{PT}

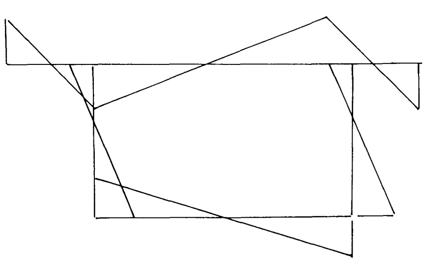

Fig. 12. Normal warping, f_w

A comparison of the stiffness K_T for typical open/closed box sections[1] indicates that $K_{T_{closed}} = 10^4 \times K_{T_{open}}$. Thus, if one can structurally close a box section, tremendous torsional stiffness can be achieved.

The induced shearing stresses are given by

$$\tau_{PT} = \frac{T_{PT}t}{K_T} \tag{23}$$

where t = plate thickness of any element.

Warping Torsion—When a thin-walled section is subjected to torsional loading, the elements do not retain their shape and thus warp. This warping will induce normal stresses and shearing stress, which can be substantially significant in open sections. The general warping normal stress is

$$f_w = BiW_n / I_w \tag{24}$$

and warping shear is given by

$$\tau_w = \frac{ES_w}{t} \phi'''$$

where

Bi = $EI_w\phi''$ = warping moment or bimoment
W_n = normalized warping function
I_w = warping constant
ϕ = total angle of rotation, radians
S_w = warping statical moment

These three induced stresses, for a closed box, are shown in Figs. 11–13.

Limiting Effects—The determination of all stresses in a curved box is difficult, due to bending and torsion interaction. Thus, it would be desirable to determine if it is necessary to evaluate both warping and pure torsional stresses in a box girder bridge.

A recent study[8] has indicated that for a central angle θ between 0 and 0.5 and $\psi \geq 10 + 40\theta$, warping can be disregarded; for θ between 0.5 and 1.0 and $\psi \geq 30$, warping is negligible, where $\psi = L[GK_T/EI_w]^{1/2}$. A study of many curved bridge systems and their respective ψ parameters, as shown in Fig. 14, shows that for single closed box units, $\psi \geq 30$; thus warping can be disregarded, providing the section is closed.

Pure torsional stress can be disregarded when $\psi \leq 0.4$.

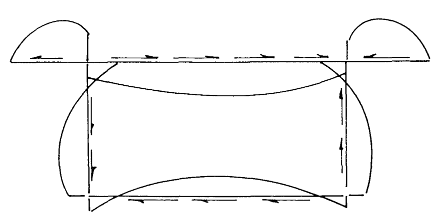

Fig. 13. Warping shear, τ_w

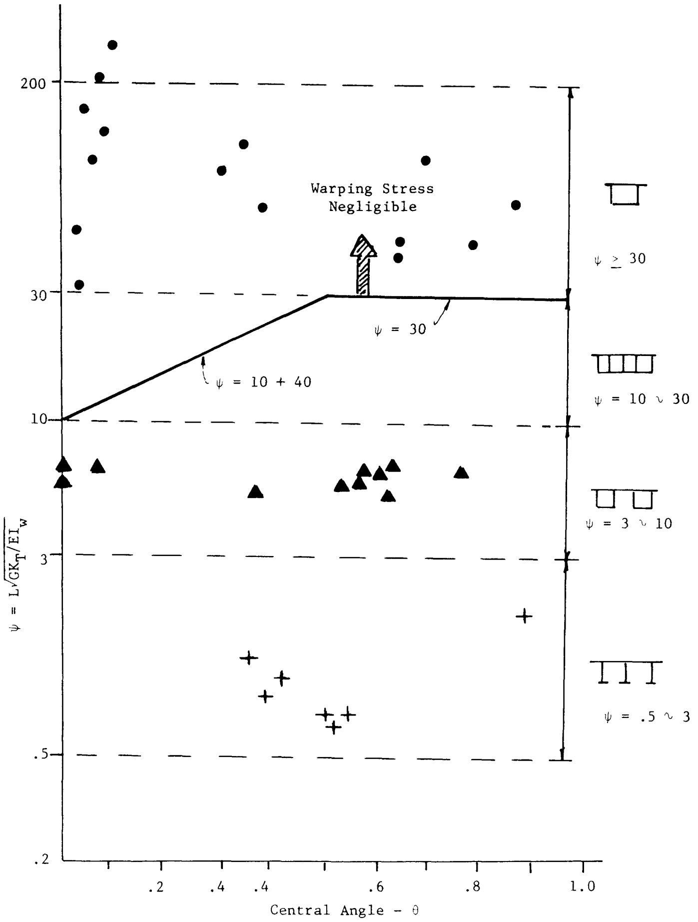

Figure 14

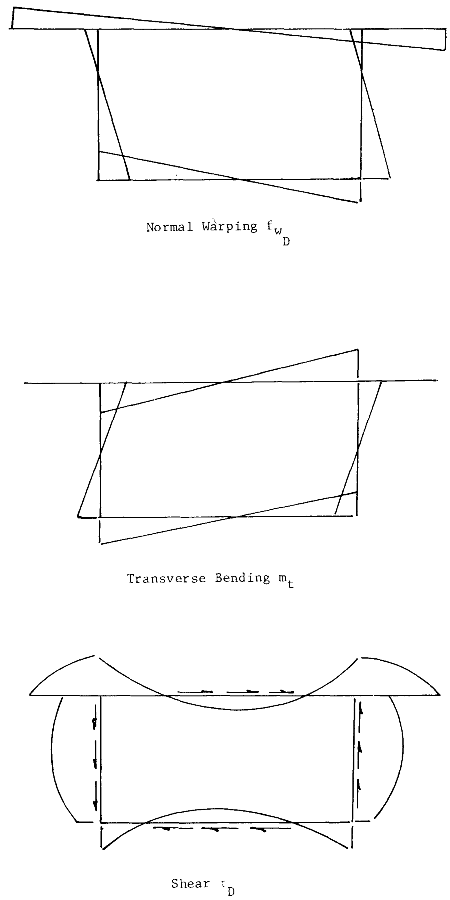

Fig. 16. Distortional stresses

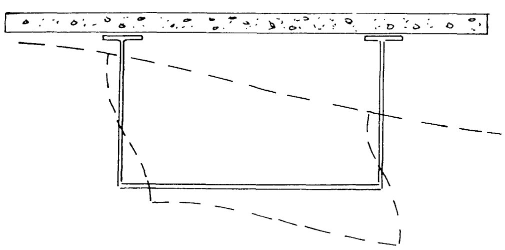

Fig. 15. Shear distortion

DISTORTIONAL STRESSES

In the development of the general torsional equations, it is assumed that the section retains its shape during deformation and final stress evaluation. However, when a box section is subjected to torsional loadings, its cross section does not retain its shape,[9,12] as shown in Fig. 15. Such a response will create additional stress in the section and will include a normal stress, a shearing stress, and a corner bending moment, as shown in Fig. 16. In order to inhibit such a response, internal diaphragms can be used[5] and thus minimize the stress development.

The required spacing and size of such bracing will be discussed in the next section.

BRACING

Top Lateral Bracing—As discussed in the section on Bending and Torsional Stresses, the torsional stiffness K_T can be substantially increased if a box section is completely closed. Examination of Figs. 17 and 18 shows a box section with top lateral bracing. This bracing can be converted[9] into an equivalent thickness by the following equation:

$$t_{eq} = \frac{E}{G}\frac{2A_d}{b}\cos^2\alpha \sin\alpha \qquad (25)$$

A study of various curved box elements, subjected to induced bending and warping normal stresses, has indicated that for $1 \leq b/d \leq 3$ (width of box to depth of box) and a stress ratio $\leq 10\%$, $t_{eq} \leq 0.050$ in., as shown in Fig. 19.

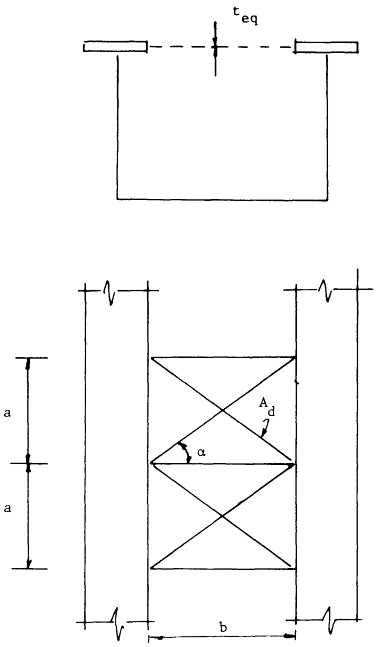

Fig. 17. Top lateral bracing

Thus, the bracing area required would be:

$$A_d(\text{in.}^2) \geq 0.03b$$

where b = bottom flange width, in.

In addition to minimizing the warping stress, the section becomes closed and thus $\psi \geq 10$, which also satisfies the warping criteria.

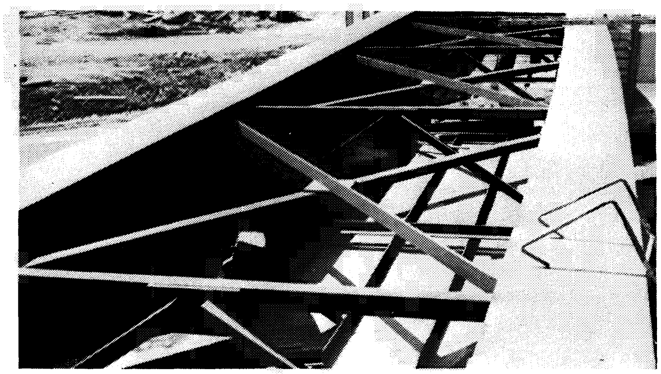

Fig. 18. Top lateral bracing

Diaphragm Bracing—As indicated previously, the minimization of normal stresses due to distortion can be achieved by placement of internal cross-diaphragms, shown in Fig. 20. A study by Heins and Olenik[5], using the typical sections shown in Tables 7 and 8, has resulted in the following general equation:

$$\frac{f_d}{f_b} = \frac{(10L - 350)}{R} \frac{S^2}{L^2} \tag{27}$$

where

f_d = induced dead load distortional normal stress
f_b = induced dead load bending normal stress
L = span length, ft
R = radius, ft
S = diaphragm spacing, ft

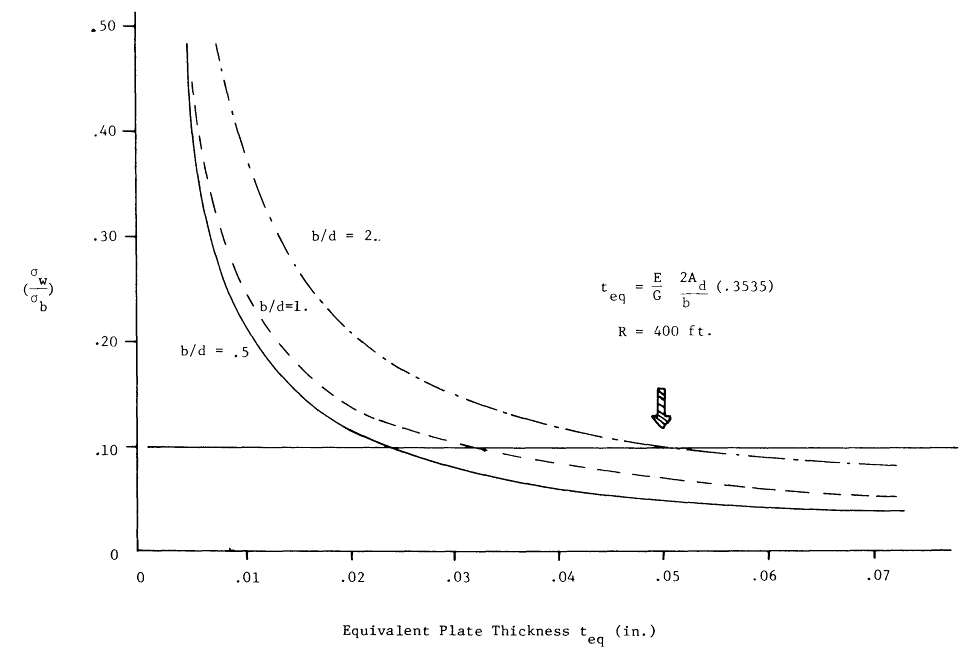

Fig. 19. Warping ratio vs. equivalent plate thickness

Fig. 20. Internal diaphragms

Examination of the induced live load ratio effect gives:

$$\left(\frac{f_d}{f_b}\right)_{LL} = \frac{3}{4}\left(\frac{f_d}{f_b}\right)_{DL} \tag{28}$$

where subscripts LL and DL represent live load and dead load, respectively.

Combining Eqs. (27) and (28) and permitting a maximum stress ratio of 10%, required diaphragm spacing is:

$$S \leq L\left(\frac{R}{200L - 7500}\right)^{1/2} \leq 25 \text{ ft} \tag{29}$$

The effect of the diaphragm stiffness, Q, on the induced distortion stress[10] is shown in Fig. 21. For $Q \geq 100$, the induced distortional stress does not change, indicating a rigid diaphragm. Therefore, setting $Q = 100$ and solving for

$$A_b = \frac{Qb\cos\alpha}{2\,Ed^2} \cdot \frac{K_1 S}{E}$$

gives

$$A_b = 75\,\frac{Sb}{d^2}\,\frac{t_w{}^3}{(d+b)} \tag{30}$$

where

A_b = area of one diagonal brace, in.
S = diaphragm spacing, in.
d = depth of box, in.
b = width of box, in.
α = angle between diagonal brace and horizontal (Fig. 21)
t_w = web thickness, in.
$\dfrac{K_1}{E} \cong \dfrac{2\,t_w{}^3}{(d+b)}$ (Ref. 9)

DESIGN SPECIFICATION

As of this date, the AASHTO specifications pertain only to straight box girders. There is, however, a set of specifications available to the engineer, which have been developed during a comprehensive project[11] called CURT. These specifications relate to both curved I and box girder bridges and refer to the current AASHTO specifications as needed.

A summary of these proposed specifications is given in Table 11. Examination of this table shows the similarity to the present straight box girder design criteria.

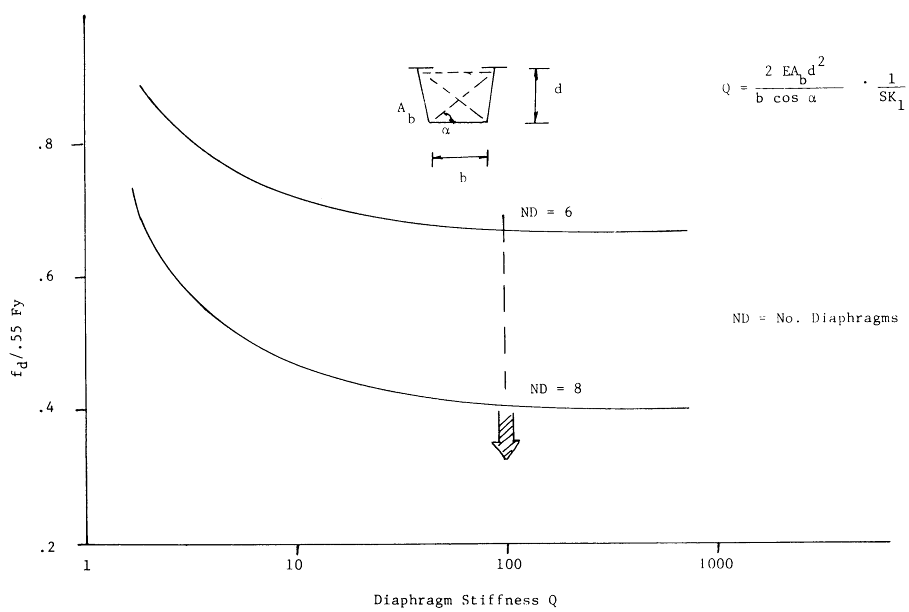

Fig. 21. Distortional stress vs. diaphragm stiffness

Table 11. Summary of Proposed Design Specifications (Ref. 11)

Item	Curved I Girder	Curved Box Girder	
Compression Flange	$F_b = 0.55\,F_y\left[1 - \frac{(l/r)^2F_y}{4\pi^2E}\right]\rho_B\rho_W$ (Note: See Table 12 for values of $\rho_B\rho_W$.)		
	$b/t \le 4400/\sqrt{F_y}$	Positive moment region: $b/t \le 4400/\sqrt{F_y}$ Negative moment region: $b/t \le (6140/F_y)X$ $X = 1 + \frac{4}{3}\left(\frac{f_v}{F_y} - 0.15\right) \ge 1.0$	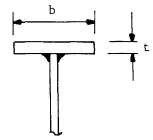
		Bottom flange: $I_s = \phi t^3 w$ $\phi = 0.07\,k^3n^4$ for $n > 1$ $= 0.125k^3$ for $n = 1$ k = buckling coefficient ≤ 4 n = number of longitudinal stiffeners k_b, k_s = buckling coefficient for compression and shear, respectively, where $4 \ge k_b \ge 2$ For flange (including stiffeners) having an allowable stress same as for tension flange: $\frac{w}{t} \le \frac{3070\sqrt{k}}{\sqrt{F_y}}X_1$ $X_1 = 1$ for $n = 1$ $= 0.93 + \left(1.6 - \frac{k}{k_s}\right)\left(\frac{f_v}{F_y}\right) \ge 1.0$ for $n > 1$ $k_s = \frac{5.34 + 2.84\sqrt[3]{I_s/wt^3}}{2(n+1)} \le 5.34$ If $\frac{w}{t} >$ above, but $\le \frac{6650\sqrt{k}}{\sqrt{F_y}}X_2$ or 60: $F_b = \left[0.326F_y + 0.224F_y\sin(\pi/2)\left(\frac{6650\sqrt{k}X_2 - (w/t)\sqrt{F_y}}{6650\sqrt{k}X_2 - 3070\sqrt{k}X_1}\right)\right]C$ $C = \sqrt{1 - 9.0\,(f_v/F_y)^2}$ $X_2 = 1 - 2.13\left(\frac{f_v}{F_y}\right) + 0.1\left[\left(\frac{k_b}{k_s}\right) - 5.34\right]^2\left(\frac{f_v}{F_y}\right)$ If $\frac{w}{t} > \frac{6650\sqrt{k}}{F_y}X_2$, but < 60: $F_b = 14.4k(t/w)^2\,C \times 10^6$ or $F_b = \left[14.4k\left(\frac{t}{w}\right)^2 \times 10^6\right] - \frac{f_v^{\,2}k}{14.4k_s^{\,2}(t/w) \times 10^6}$ whichever is smaller	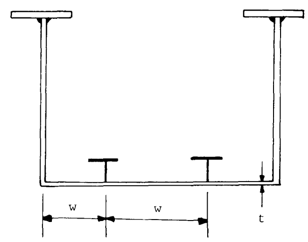
Tension Flange	$f_w + f_b \le 0.55\,F_y$	$F_b = 0.55F_y[1 - 9.2\,(f_v/F_y)^2]^{1/2}$ $f_v \le 0.33F_y$	
Web Plate (No longitudinal stiffeners)	For $d_o/R \le 0.02$: Use AASHTO Spec. Art. 1.7.70(A). For $d_o/R > 0.02$: $t \ge \frac{D\sqrt{f_b}}{23{,}000}(\psi)$ but not less than $D/170$ $\psi = 1.19 - 10(d_o/R) + 34(d_o/R)^2$ where d_o = actual distance between transverse stiffeners, in. R = radius of girder curvature, in.		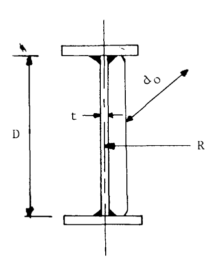

(cont'd next page)

Table 11 (cont'd). Summary of Proposed Design Specifications (Ref. 11)

Item	Curved I Girder	Curved Box Girder	Detail
Web Plate (Single longitudinal stiffener)	$t = \frac{D\sqrt{f_b}}{46{,}000}\left(\frac{1}{\psi}\right)$ but not less than $D/340$ $\psi = 1 - 2.9\left(\frac{d_o}{R}\right)^{1/2} + 2.2\left(\frac{d_o}{R}\right)$		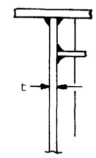
Web Plate (Transverse intermediate stiffeners)	AASHTO Spec. Art. 1.7.71 applies, except $I_s \geq d_o t^3 J/10.92$ $J = [(25D^2/d^2) - 20]X \geq 5$ $X = \frac{1.0 + [(d/D) - 0.78]Z^4}{1775}$ when $0.78 \leq d/D \leq 1.0$ and $0 \leq Z \leq 10$ $d \leq 11{,}000\ t/\sqrt{f_v}$ (req'd spacing of stiffeners) $Z = 0.95d^2/Rt$ Note: If $t \geq D\sqrt{f_v}/7500$, no stiffener req'd.		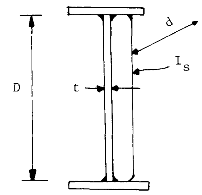
Longitudinal Stiffeners	$I_s = Dt^3\left[2.4\left(\frac{d_o^2}{D^2}\right) - 0.13\right]$ $t_s = b'\sqrt{f_b}/2250$ $r \geq d_0\sqrt{F_y}/23{,}000$ where I_s = moment of inertia of stiffener r = radius of gyration of stiffener Note: In computing I_s and r, a centrally located web strip $\leq 18t$ shall be considered as part of the longitudinal stiffener.		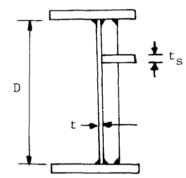 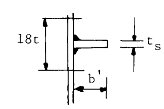
Shear Connectors	P_c = force on a connector $= \left(\overline{P}^2 + F^2 + 2\overline{P}F\sin\frac{\theta}{2}\right)^{1/2} \leq \phi S_u$ $\phi = 0.85$ S_u = ultimate strength of connector [see AASHTO Spec. Art. 1.7.100 (A) (2)] $\overline{P} = P/N$ N = no. of conn. between pts. of max. pos. moment and adjacent end supports or dead load points of contraflexure, or between pts. of max. neg. moment and adjacent dead load points of contraflexure P = $0.85f'_c bc$ or A_sF_y [whichever is smaller at pts. of max. pos. moment. At pts. of neg. moment, see AASHTO Spec. Art. 1.7.100 (A)(2)] $F = \frac{P(1-\cos\theta)}{4KN_s\sin(\theta/2)}$ θ = angle subtended between pt. of max. moment (pos. or neg.) and adjacent pt. of contraflexure or support $K = 0.166\left(\frac{N}{N_s} - 1\right) + 0.375$ A_s = total area of steel section, incl. cover plates		

Table 12. Curvature Reduction Factor $\rho_B \rho_W$ for Allowable Stress

$\frac{l}{R}$	$\frac{f_w}{f_b}$	l/b										
		7	8	9	10	12	14	16	18	20	22	24
	0.50	0.74	0.75	0.75	0.75	0.75	0.76	0.76	0.76	0.77	0.77	0.77
	0.25	0.84	0.84	0.35	0.85	0.85	0.85	0.86	0.86	0.87	0.87	0.87
0.008	0.00	0.95	0.94	0.93	0.93	0.91	0.90	0.89	0.87	0.86	0.85	0.84
	−0.25	0.77	0.77	0.76	0.76	0.75	0.75	0.74	0.73	0.73	0.72	0.72
	−0.50	0.65	0.65	0.65	0.65	0.64	0.64	0.64	0.63	0.63	0.63	0.63
	0.50	0.74	0.74	0.74	0.74	0.74	0.74	0.74	0.74	0.74	0.75	0.75
	0.25	0.83	0.83	0.83	0.83	0.84	0.84	0.84	0.84	0.84	0.84	0.84
0.010	0.00	0.93	0.93	0.92	0.91	0.89	0.88	0.86	0.85	0.83	0.82	0.81
	−0.25	0.76	0.76	0.75	0.75	0.74	0.73	0.72	0.71	0.70	0.70	0.69
	−0.50	0.64	0.64	0.64	0.63	0.63	0.62	0.62	0.61	0.61	0.61	0.60
	0.50	0.72	0.72	0.72	0.72	0.71	0.71	0.71	0.71	0.71	0.70	0.70
	0.25	0.81	0.81	0.81	0.81	0.81	0.80	0.80	0.80	0.80	0.80	0.79
0.014	0.00	0.91	0.90	0.89	0.88	0.86	0.84	0.82	0.80	0.78	0.76	0.75
	−0.25	0.74	0.74	0.73	0.72	0.71	0.69	0.68	0.67	0.66	0.65	0.64
	−0.50	0.63	0.62	0.62	0.61	0.60	0.59	0.59	0.58	0.57	0.56	0.56
	0.50	0.71	0.70	0.70	0.70	0.69	0.69	0.68	0.68	0.67	0.67	0.66
	0.25	0.80	0.79	0.79	0.79	0.78	0.78	0.77	0.77	0.76	0.76	0.75
0.018	0.00	0.89	0.87	0.86	0.85	0.82	0.80	0.78	0.76	0.74	0.72	0.70
	−0.25	0.72	0.71	0.71	0.70	0.68	0.66	0.65	0.63	0.62	0.61	0.60
	−0.50	0.61	0.60	0.60	0.59	0.58	0.57	0.56	0.55	0.54	0.53	0.52
	0.50	0.69	0.69	0.68	0.68	0.67	0.66	0.66	0.65	0.64	0.64	0.63
	0.25	0.78	0.78	0.77	0.77	0.76	0.75	0.74	0.73	0.73	0.72	0.71
0.022	0.00	0.87	0.85	0.83	0.82	0.79	0.76	0.74	0.72	0.69	0.67	0.65
	−0.25	0.71	0.70	0.68	0.67	0.65	0.64	0.62	0.60	0.59	0.57	0.56
	−0.50	0.60	0.59	0.58	0.57	0.56	0.54	0.53	0.52	0.51	0.50	0.49
	0.50	0.68	0.67	0.67	0.66	0.65	0.64	0.63	0.63	0.62	0.61	0.60
	0.25	0.77	0.76	0.76	0.75	0.74	0.73	0.72	0.71	0.70	0.69	0.68
0.026	0.00	0.85	0.83	0.81	0.79	0.76	0.73	0.71	0.68	0.66	0.64	0.62
	−0.25	0.69	0.68	0.66	0.65	0.63	0.61	0.59	0.57	0.56	0.54	0.53
	−0.50	0.58	0.57	0.56	0.55	0.54	0.52	0.51	0.49	0.48	0.47	0.46
	0.50	0.67	0.66	0.65	0.65	0.64	0.62	0.61	0.60	0.60	0.59	0.58
	0.25	0.76	0.75	0.74	0.73	0.72	0.71	0.69	0.68	0.67	0.66	0.66
0.030	0.00	0.83	0.81	0.79	0.77	0.74	0.70	0.68	0.65	0.63	0.60	0.58
	−0.25	0.67	0.66	0.65	0.63	0.61	0.59	0.56	0.55	0.53	0.51	0.50
	−0.50	0.57	0.56	0.55	0.54	0.52	0.50	0.48	0.47	0.46	0.45	0.43
	0.50	0.64	0.63	0.62	0.62	0.60	0.59	0.57	0.56	0.55	0.54	0.53
	0.25	0.73	0.72	0.71	0.70	0.68	0.66	0.65	0.64	0.62	0.61	0.60
0.040	0.00	0.78	0.76	0.74	0.71	0.68	0.64	0.61	0.58	0.56	0.53	0.51
	−0.25	0.64	0.62	0.60	0.59	0.56	0.53	0.51	0.49	0.47	0.45	0.44
	−0.50	0.54	0.52	0.51	0.50	0.48	0.46	0.44	0.42	0.41	0.39	0.38
	0.50	0.62	0.61	0.60	0.59	0.47	0.56	0.54	0.53	0.52	0.51	0.50
	0.25	0.70	0.69	0.68	0.67	0.65	0.63	0.61	0.60	0.59	0.58	0.55
0.050	0.00	0.74	0.71	0.69	0.67	0.63	0.59	0.56	0.53	0.50	0.48	0.45
	−0.25	0.60	0.58	0.57	0.55	0.52	0.49	0.46	0.44	0.42	0.40	0.39
	−0.50	0.51	0.49	0.48	0.47	0.44	0.42	0.40	0.38	0.37	0.35	0.34

(cont'd next page)

Table 12 (cont'd).

$\frac{l}{R}$	$\frac{f_w}{f_b}$	l/b 7	8	9	10	12	14	16	18	20	22	24
	0.50	0.60	0.59	0.58	0.57	0.55	0.53	0.52	0.51	0.50	0.49	0.48
	0.25	0.68	0.67	0.66	0.64	0.62	0.60	0.59	0.57	0.56	0.52	0.49
0.060	0.00	0.70	0.68	0.65	0.63	0.58	0.54	0.51	0.48	0.45	0.43	0.41
	−0.25	0.57	0.55	0.53	0.51	0.48	0.45	0.43	0.40	0.38	0.37	0.35
	−0.50	0.48	0.47	0.45	0.44	0.41	0.39	0.37	0.35	0.33	0.32	0.31
	0.50	0.59	0.57	0.56	0.55	0.53	0.52	0.50	0.49	0.48	0.47	0.46
	0.25	0.66	0.65	0.64	0.62	0.60	0.58	0.57	0.55	0.51	0.48	0.45
0.070	0.00	0.67	0.64	0.61	0.59	0.54	0.51	0.47	0.44	0.42	0.39	0.37
	−0.25	0.55	0.52	0.50	0.48	0.45	0.42	0.39	0.37	0.35	0.33	0.32
	−0.50	0.46	0.44	0.43	0.41	0.38	0.36	0.34	0.32	0.30	0.29	0.28
	0.50	0.57	0.56	0.55	0.53	0.51	0.50	0.48	0.47	0.46	0.45	0.44
	0.25	0.65	0.63	0.62	0.60	0.58	0.56	0.55	0.51	0.47	0.44	0.41
0.080	0.00	0.64	0.61	0.58	0.56	0.51	0.47	0.44	0.41	0.38	0.36	0.34
	−0.25	0.52	0.50	0.48	0.46	0.42	0.39	0.37	0.34	0.33	0.31	0.29
	−0.50	0.44	0.42	0.40	0.39	0.36	0.34	0.31	0.30	0.28	0.27	0.26
	0.50	0.56	0.54	0.53	0.52	0.50	0.48	0.46	0.45	0.44	0.43	0.42
	0.25	0.63	0.61	0.60	0.58	0.56	0.54	0.51	0.47	0.44	0.41	0.38
0.090	0.00	0.61	0.58	0.55	0.53	0.48	0.44	0.41	0.38	0.36	0.34	0.32
	−0.25	0.50	0.48	0.45	0.43	0.40	0.37	0.34	0.32	0.30	0.29	0.27
	−0.50	0.42	0.40	0.38	0.37	0.34	0.31	0.29	0.28	0.26	0.25	0.24
	0.50	0.54	0.52	0.51	0.49	0.47	0.45	0.44	0.43	0.41	0.40	0.40
	0.25	0.61	0.59	0.57	0.56	0.53	0.51	0.48	0.44	0.41	0.38	0.35
0.100	0.00	0.59	0.56	0.53	0.50	0.45	0.42	0.38	0.36	0.33	0.31	0.29
	−0.25	0.48	0.45	0.43	0.41	0.38	0.35	0.32	0.30	0.28	0.27	0.25
	−0.50	0.40	0.38	0.37	0.35	0.32	0.30	0.28	0.26	0.24	0.23	0.22

COMPUTER SOLUTION

Theory—The general load deformation response of a curved girder, which may have an arbitrary geometry when subjected to combined vertical (q_y), lateral (q_x), longitudinal (q_z), and moment (m_z) uniform loads applied along the girder, as shown in Fig. 22, is given by the following differential equations, as developed by Vlasov.[13]

$$\left(\frac{EI_w}{R^2} - EI_x\right) \eta^{iv} + \frac{GK_T}{R^2} \eta'' - \frac{EI_w}{R} \phi^{iv} + \frac{EI_x}{R} \phi'' + q_y = 0 \quad (31)$$

$$-\frac{EI_w}{R} \eta^{iv} + \frac{EI_x + GK_T}{R} \eta'' - EI_w \phi^{iv} + GK_T \phi'' - \frac{EI_x}{R^2} \phi + m_z = 0 \quad (32)$$

where

η = vertical deflection along girder (y-axis)
ϕ = transverse rotation of girder (about z-axis)
EI_x = primary bending stiffness
GK_T = torsional stiffness
EI_w = warping stiffness
R = radius to center line of box

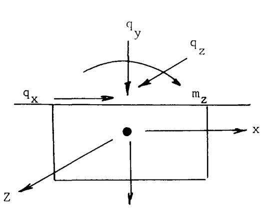

Fig. 22. Box girder forces

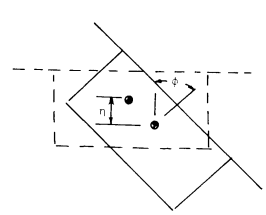

Fig. 23. Box girder displacements

$$\left[\boxed{\begin{matrix}\frac{EI_w}{R^2}+EI_x\\[2ex] \frac{EI_w}{R}\end{matrix}}\ \boxed{\begin{matrix}-\left[4\left(\frac{EI_w}{R^2}+EI_x\right)+\frac{\Delta^2 GK_T}{R^2}\right]\\[2ex] -\left[4\left(\frac{EI_w}{R}\right)+\frac{\Delta^2(EI_x+GK_T)}{R}\right]\end{matrix}}\ \boxed{\begin{matrix}6\left(\frac{EI_w}{R^2}+EI_x\right)+\frac{2\Delta^2 GK_T}{R^2}\\[2ex] 6\left(\frac{EI_w}{R}\right)+\frac{2\Delta^2(EI_x+GK_T)}{R}\end{matrix}}\ \boxed{\begin{matrix}-\left[4\left(\frac{EI_w}{R^2}+EI_x\right)+\frac{\Delta^2 GK_T}{R^2}\right]\\[2ex] -\left[4\left(\frac{EI_w}{R}\right)+\frac{\Delta^2(EI_x+GK_T)}{R}\right]\end{matrix}}\ \boxed{\begin{matrix}\frac{EI_w}{R^2}+EI_x\\[2ex] \frac{EI_w}{R}\end{matrix}}\right]\begin{matrix}\eta\\[2ex] \phi\end{matrix} = q_y\Delta^4 \quad (33)$$

LL L O R RR

$$\left[\boxed{\begin{matrix}\frac{EI_w}{R}\\[2ex] EI_w\end{matrix}}\ \boxed{\begin{matrix}-\left[4\left(\frac{EI_w}{R}\right)+\frac{\Delta^2(EI_x+GK_T)}{R}\right]\\[2ex] -|4(EI_w)+\Delta^2 GK_T|\end{matrix}}\ \boxed{\begin{matrix}6\left(\frac{EI_w}{R}\right)+\frac{2\Delta^2(EI_w+GK_T)}{R}\\[2ex] 6(EI_w)+2\Delta^2 GK_T+\frac{\Delta^4 EI_x}{R^2}\end{matrix}}\ \boxed{\begin{matrix}-\left[4\left(\frac{EI_w}{R}\right)+\frac{\Delta^2(EI_x+GK_T)}{R}\right]\\[2ex] -|4(EI_w)+\Delta^2 GK_T|\end{matrix}}\ \boxed{\begin{matrix}\frac{EI_w}{R}\\[2ex] EI_w\end{matrix}}\right]\begin{matrix}\eta\\[2ex] \phi\end{matrix} = m_z\Delta^4 \quad (34)$$

Figure 24

The displacements of the box are shown in Fig. 23. These equations have been solved simultaneously by writing the differentials in central finite difference form.[4,7] The mesh spacing between nodes is defined as Δ, resulting in Eqs. (33) and (34), as shown in Fig. 24. The general mesh patterns are appropriately modified to accommodate exterior (simple or fixed) supports in bending or torsion and interior supports.

The deformations η and ϕ at each node are then used to evaluate internal forces, as given by Eqs. (35) through (38), defined by Vlasov:[13]

$$M_x = -EI_x\left(\eta'' - \frac{\phi}{R}\right) \quad (35)$$

$$Bi = -EI_w\left(\phi'' + \frac{\eta''}{R}\right) \quad (36)$$

$$M_{ST} = GK_T\left(\phi' + \frac{\eta'}{R}\right) \quad (37)$$

$$M_w = -EI_w\left(\phi''' + \frac{\eta'''}{R}\right) \quad (38)$$

where

M_x = primary bending moment
Bi = bimoment (warping normal stress function)
M_{ST} = pure torsional moment
M_w = warping moment

Equations (35) through (38) have also been written in finite difference notation, thus permitting evaluation of the forces upon determination of deformations.

The primary normal stresses induced into the box are then computed by the classic equations given in the section "Bending and Torsional Stresses."

Distortion of Curved Sections—In the previous section, the load-deformation equations were developed on the premise that the box cross section retains its shape. As described in the discussion of "Distortional Stresses", it is known that the cross section distorts. The load-deformation response of such a box is given by the following differential equation, as developed by Dabrowski:[9]

$$\gamma^{iv} + 4\lambda^4\gamma = \frac{1}{WA^*}\left(\rho\frac{M_x}{R} + \frac{m_z}{2}\right) \quad (39)$$

where

γ = angular distortion of box section
M_x = internal primary bending moment [Eq. (35)]
R = radius to center line of box
WA^*, ρ, λ = geometric properties of box
m_z = external torsional loading per length (as previously described)

The solution of Eq. (39) can readily be performed by converting the differential into finite difference form, giving Eq. (40):

$$(1)(-4)(6 + 4\lambda^4\Delta^4)(-4)(1) = \frac{\Delta^4}{WA^*}\left(\rho\frac{M_x}{R} + \frac{m_z}{2}\right) \quad (40)$$

This equation is appropriately modified to consider interior diaphragms or supports by assuming $\gamma = 0$. In evaluating Eq. (40), the internal bending moment M_x is required in addition to the external torsional moment m_z. Thus, the primary analysis is first conducted to determine M_x; then the distortional analysis is performed. If interior transverse diaphragms are imposed, thus inhibiting distortional behavior, γ at that location is assumed to be zero.

The induced normal stress due to distortion of the cross section is given by:

$$\sigma_f = -\gamma'' A^* \cdot \tilde{W} \quad (41)$$

where

γ'' = second derivative of angular distortion computed in difference form
$A^*, \tilde{W}$ = cross-sectional properties

All of the above equations have been incorporated into a computer program which will now be described.

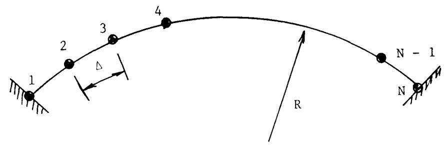

Fig. 25. Nodal point configurations

Computer Program—As has been previously mentioned, the governing differential equation for cross-sectional distortion was solved using the finite difference numerical technique. Also noted was the need for the values of the independent variable M_x prior to solving Eq. (39); therefore, the equations for torsion and bending of curved girders must first be determined. This was done using an existing computer program,[6] which utilizes the finite difference method to solve the differential equations, as previously described. Once the values for the vertical displacements, η, and the rotations, ϕ, have been obtained, they and their appropriate derivatives are substituted into Eq. (35) to determine the values for the induced bending moments. The values for the bending moments are then transferred to a subroutine that has been written to carry out the distortional analysis. Finally, from this subroutine the values for the distortional stresses are obtained.

A general schematic of a curved beam used in the computer program[5,6] is shown in Fig. 25.

The computer program stores the banded coefficient array in a rectangular matrix to economize on the storage locations required. The resulting augmented matrix is solved using a decomposition method. If a diaphragm is to be located at an arbitrary node point i, the angular distortion at this point is assumed to be equal to zero. In order to make the equations compatible with this assumption, the i^{th} row and corresponding diagonal of the coefficient array, as well as the i^{th} term of the load array, must be eliminated from the augmented matrix. After the appropriate terms have been eliminated, the augmented matrix is then condensed. The above procedure was performed at each diaphragm location before the equations were solved for the unknown angular distortions between the diaphragms.

Program Input—The general computer input data included:

a. Number of mesh points
b. Support conditions, number of interior supports
c. Material properties
d. Girder geometry
e. Radius
f. Loading (uniform or concentrated)

Program Output—The program will print out the following for each mesh-point along the girder length.

a. Vertical deflection, in.
b. Rotation, rad
c. Bending moment, kip-in.
d. Shear force, kips
e. St. Venant torque, kip-in.
f. Warping moment, kip-in.
g. Total torque, kip-in.
h. Bimoment, kip-in.^{2}
i. Angular distortion, rad
j. Normal bending stresses, ksi
k. Normal warping stresses, ksi
l. Normal distortional stresses, ksi

A new version of the box beam program is being developed and will accommodate continuous spans, automatic dead and live load generation, influence lines, force envelopes (M, V, Bi, T) and selection of plate size according to the specifications given in Table 11.

REFERENCES

1. *Hall, D. H. et al.* Horizontally Curved Steel Box Girder Bridges—A Survey *Task Committee on Curved Box Girders, ASCE-AASHTO Committee on Flexural Members, Committee on Metals, Structural Division, ASCE (to be published).*
2. *American Association of State Highway and Transportation Officials* Standard Specifications for Highway Bridges *11th Edition, 1973.*
3. *Mattock, A. H. and S. B. Johnston* An Experimental and Analytical Study of the Lateral Distribution of Load in Composite Box Girder Bridges *Final Report, U.S.S. Corp., Pittsburgh, Pa., 1968.*
4. *Heins, C. P. and J. C. Oleinik* Curved Box Beam Bridge Analysis *Computers and Structures Journal, Vol. 6, pp. 65–73, Pergamon Press, London, 1976.*
5. *Oleinik, J. C. and C. P. Heins* Diaphragms for Curved Box Beam Bridges *ASCE Journal of the Structural Division, Vol. 101, No. ST10, Oct. 1975.*
6. *Oleinik, J. C. and C. P. Heins* Diaphragm Spacing Requirements for Curved Steel Box Beam Bridges *Civil Engineering Report No. 58, University of Maryland, College Park, Md., Aug. 1974.*
7. *Heins, C. P.* Bending and Torsional Design of Structural Members *Lexington Books, Lexington, Mass., 1975.*
8. *Nakai, H. and C. P. Heins* Analysis Criteria for Curved Bridges *ASCE Journal of the Structural Division, Vol. 103, No. ST7, July 1977.*
9. *Dabrowski, R.* Curved Thin Walled Girders *Cement and Concrete Association, London, England 1968.*
10. *Williamson, D. M.* BEF Analysis for Cross-Sectional Deformation of Curved Box Girders with Internal Diaphragms *M.S. THESIS= Civil Engr. Dept., Carnegie-Mellon University, Pittsburgh, Pa., April 1974.*
11. Tentative Design Specifications for Horizontally Curved Highway Bridges *Final Report, CURT—Project HPR2-(111), March, 1975.*
12. *Mozer, J. D. and C. G. Culver* Behavior of Curved Box Girders—Laboratory Observations *ASCE Specialty Conference on Metal Bridges, St. Louis, Mo., Nov. 12–13, 1974.*
13. *Vlasov, V.* Thin Walled Beam Theory *NSF, Washington, D.C., 1961.*